Article

Ultrasensitive Photoelectrochemical Assay with PTB7-Th/CdTe QDs Sensitized Structure as Signal Tag and 4-CD Precipitate as Efficient Quencher

Mengjie Li, Xin Tian, Wen-Bin Liang, Ruo Yuan, and Yaqin Chai

Anal. Chem., **Just Accepted Manuscript** • DOI: 10.1021/acs.analchem.8b04370 • Publication Date (Web): 16 Nov 2018

Ultrasensitive Photoelectrochemical Assay with PTB7-Th/CdTe QDs Sensitized Structure as Signal Tag and 4-CD Precipitate as Efficient Quencher

Mengjie Li, Xin Tian, Wenbin Liang, Ruo Yuan*, Yaqin Chai*

Key Laboratory of Luminescent and Real-Time Analytical Chemistry (Southwest University), Ministry of Education, College of Chemistry and Chemical Engineering, Southwest University, Chongqing 400715, PR China.

* Corresponding author. Tel.: +86-23-68252277; Fax: +86-23-68253172.

E-mail address: yuanruo@swu.edu.cn (R.Yuan), yqchai@swu.edu.cn (Y. Q. Chai)

Abstract

Herein, an ultrasensitive photoelectrochemical (PEC) assay was developed for the monitoring of microRNA-141 (miRNA-141) based on poly{4,8-bis[5-(2-ethylhexyl)thiophen-2-yl]benzo[1,2-b:4,5-b′]dithiophene-2,6-diyl-alt-3-fluoro-2-[(2-ethylhexyl)-carbonyl]thieno[3,4-b]thiophene-4,6-diyl} (PTB7-Th)/ CdTe quantum dots (CdTe QDs) sensitized structure as signal tag and the benzo-4-chloro-hexadienone (4-CD) precipitate as efficient quencher. PTB7-Th and CdTe QDs were successively modified on electrode surface to form a novel sensitized structure with eminent photovoltaic performances and surpassing film-forming ability. The PTB7-Th/CdTe QDs sensitized structure was served as signal tag for achieving a strong initial PEC signal. Besides, a tiny amount of target (miRNA-141) could be transformed into numerous DNA product *via* enzyme-assisted target cycling procedure, which further triggered the formation of DNA supersanwich structure on electrode surface for loading abundant manganese porphyrin (MnPP). Thereafter, MnPP as mimetic enzyme could catalyze 4-chloro-1-naphthol (4-CN) to generate 4-CD precipitate on sensing interface in the presence of H_2O_2, which could efficiently block electron transfer, leading to a significantly quenched PEC signal for determination of miRNA-141. The designed PEC biosensor performed a wide detection range from 0.1 fM to 1 nM with a low detection limit of 33 aM for miRNA-141, which paved a new avenue for highly accurate and ultrasensitive monitoring of multifarious analytes in bioanalysis and clinical diagnosis.

Introduction

Photoelectrochemical (PEC) assay with handy operation, low background noise and high sensitivity has aroused enormous concern over recent years.[1-3] In routine PEC analysis systems, electron donors including hydrogen peroxide (H_2O_2), ascorbic acid and dopamine are directly added into electrolyte solution to neutralize the photogenerated holes for achieving steady and favorable PEC signal.[4-8] Nevertheless, in this case, the electron transport process between the electron donor and the photoactive material is an intermolecular electron transport process, which would lead to the restricted photoelectric conversion efficiency. Recently, the donor-acceptor (D-A) type photoactive materials have gained great research interest, which is attributed to the fact that they can realize the intramolecular electron transport process, thereby reducing the energy loss during electron transmission and improving the photoelectric conversion efficiency.[9, 10] Among diverse D-A type photoactive materials, poly{4,8-bis[5-(2-ethylhexyl)thiophen-2-yl]benzo[1,2-b:4,5-b′]dithiophene -2,6-diyl-alt-3-fluoro-2-[(2-ethylhexyl)-carbonyl]thieno[3,4-b]thiophene-4,6-diyl}(PT B7-Th) is a particularly outstanding member because of its excellent film-forming ability and photoelectric properties.[11-13] Currently, we employed PTB7-Th as photoactive material, fullerene[12] or polyaniline[13] as sensitizer to construct sensitive PEC biosensors. Although analytical performances of the above PTB7-Th-based PEC biosensors have been improved, the preparation and immobilization of the corresponding sensitizers are very difficult. Therefore, it's urgently essential to seek an easily prepared and highly efficient sensitizer to enhance the PEC signal of

PTB7-Th for constructing sensitive biosensor. Herein, CdTe quantum dots (CdTe QDs) with eminent photovoltaic performances and film-forming ability[14-16] was selected as the sensitizer to constitute a novel sensitized structure with PTB7-Th *via* convenient layer-by-layer drop-coating for achieving a strong initial PEC signal.

In recent years, nucleic acid-based signal amplification technology has been extensively applied in biosensor field for obtaining high detection sensitivity.[17-21] Among diverse nucleic acid amplification approaches, enzyme-assisted target cycling amplification strategy with extremely high specificity and selectivity is a particularly excellent amplification method.[20, 21] Compared with the traditional 1:1 ratio pattern, it could achieve a target-to-product DNA ratio of 1:n, leading to significant signal amplification.[22] Besides, DNA supersanwich structure possesses a long double-strand DNA structure, which also demonstrates great potential in signal amplification.[23, 24] In view of these merits, combining enzyme-assisted target cycling amplification with DNA supersanwich structure is highly promising for improving detection sensitivity. Hence, duplex specific nuclease (DSN) enzyme-assisted target cycling procedure was adopted in this work, which could transform a tiny amount of target (miRNA-141) into numerous DNA product. The DNA product would trigger the formation of DNA supersanwich structure for loading abundant mimetic enzyme, thereby realizing biocatalytic precipitation reaction and resulting in a significantly quenched PEC signal. Accordingly, high sensitive detection of miRNA-141 could be expected on the basis of the dual amplification strategy and the high quenching efficiency of 4-CD toward PTB7-Th/CdTe QDs sensitized structure.

Herein, a novel PEC biosensor was created based on PTB7-Th/CdTe QDs sensitized structure as signal tag and biocatalytic reaction products (benzo-4-chloro-hexadienone, 4-CD) as efficient quencher for ultrasensitive monitoring of miRNA-141. As depicted in Scheme 1, the D-A type photoactive material PTB7-Th and the sensitizer CdTe QDs were continuously coated on electrode interface, therefrom forming a novel sensitized structure. The obtained PTB7-Th/CdTe QDs sensitized structure was served as the signal tag, which could lead to a strong initial PEC signal without any additional electron donors. Moreover, enzyme-assisted target cycling procedure could transform target into numerous DNA product, and then the DNA product would trigger the formation of DNA supersanwich structure with the aid of S1 and S2 for intercalating abundant mimetic enzymes manganese porphyrin (MnPP). Ultimately, in the presence of H_2O_2, MnPP catalyzed 4-chloro-1-naphthol (4-CN) oxidation to generate benzo-4-chloro-hexadienone (4-CD) precipitate on sensing interface. The produced 4-CD as efficient quencher could block the electron transmission path between the photoactive material and the electrolyte solution, resulting in a prominently depressed PEC signal. Consequently, the designed PEC analysis strategy could quantitatively detect the miRNA-141 concentration with great accuracy and high sensitivity. The successful construction of this PEC assay revealed a new platform for bioanalysis and clinical diagnosis with high accuracy and sensitivity.

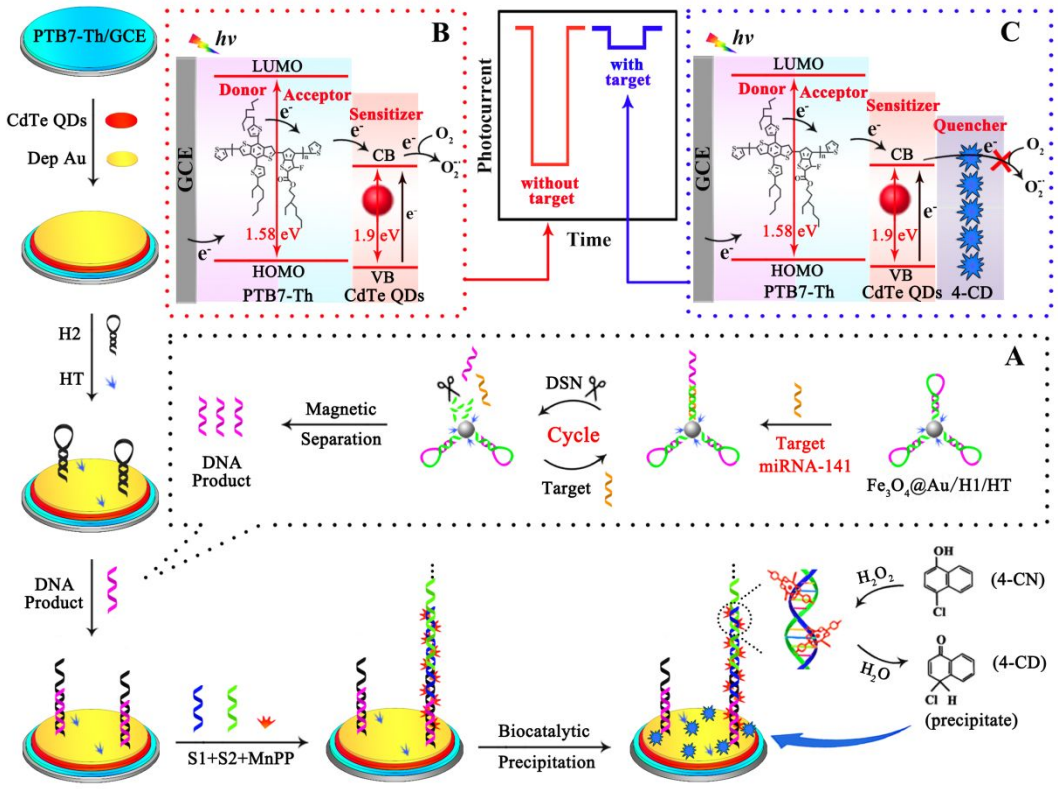

Scheme 1. Schematic illustration of the proposed PEC assay for miRNA-141 detection. (A) DSN enzyme-assisted target cycling procedure. The mechanism of electron transfer for photocurrent generation (B) and photocurrent quenching (C).

Experimental Section

Preparation of CdTe QDs, Fe_3O_4@Au and PTB7-Th Solution

CdTe QDs and Fe_3O_4@Au were prepared based on the protocols reported previously.[25, 26] For preparation of PTB7-Th solution, 1 mg PTB7-Th was added into 3 mL chloroform with ultrasonication until homogeneous blackish green solution appeared. The acquired PTB7-Th solution was kept in a refrigerator before use.

DSN Enzyme-Assisted Target Cycling Procedure

The target cycling procedure with the assistance of DSN enzyme was illustrated in Scheme 1A. Briefly, 200 μL Fe_3O_4@Au was mixed with 200 μL 2 μM H1 under

stirring for 14 h. Next, Fe_3O_4@Au/H1 was acquired *via* magnetic separation, and then redispersed in 200 μL ultrapure water. Subsequently, 20 μL 0.1 mM hexanethiol (HT) was added for blocking nonspecific adsorption sites. After that, 0.5 μL 1 U DSN enzyme, 0.5 μL 1 × DSN master buffer and 50 μL miRNA-141 (target) were added simultaneously and reacted at 60 °C for 40 min. Afterward, DSN enzyme was denatured through injecting DSN stop solution (5 μL) into the mixture solution. Ultimately, the converted DNA sequence (DNA product) was separated *via* magnetic force and employed for hybridizing with H2 on electrode surface.

Fabrication of the PEC Biosensor

The mirror-like glassy carbon electrode (GCE) was acquired through the method reported previously.[21] 10 μL PTB7-Th and 10 μL CdTe QDs were coated on GCE surface gradually, followed by drying at 37 °C. After electrodepositing in 1% $HAuCl_4$ solution (DepAu) for 15 s, the gold nanoparticles layer was attached on the CdTe QDs/PTB7-Th/GCE surface. Then 15 μL 2 μM H2 was coated on the DepAu/CdTe QDs/PTB7-Th/GCE surface for reacting 14 h at 4 °C. Next, HT (10 μL, 0.1 mM) as the blocking agent was incubated for 0.5 h at 25 °C. After incubating 15 μL DNA product for 2 h, 5 μL 100 μM MnPP, 10 μL 2 μM S1 and 10 μL 2 μM S2 were dropped simultaneously and reacted at 37 °C for 2 h, leading to form DNA supersanwich structure for loading massive MnPP. Ultimately, the 4-CD precipitate was produced on the acquired electrode surface after incubating of 0.15 mM H_2O_2 and 1 mM 4-CN for 15 min, which was attributable to the mimetic enzyme (MnPP) biocatalytic precipitation reaction.[27, 28] The fabrication of PEC biosensor was

exhibited in Scheme 1.

Results and Discussion

Characterizations of PTB7-Th and CdTe QDs

Scanning electron microscopy (SEM), high-resolution transmission electron microscopy (HRTEM) and UV-visible (UV-vis) absorption spectroscopy were employed to characterize PTB7-Th and CdTe QDs. As observed in Figure 1A, PTB7-Th possessed a flat bedded structure and its size was about 6 μm, which was benefited from its excellent film-forming ability and high ductility. The prepared CdTe QDs exhibited clear lattice fringes and well dispersion, and their average diameter were approximately 4 nm, which was presented in Figure 1B. The UV-vis spectroscopy of PTB7-Th and CdTe QDs could be observed in Figure 1C and Figure 1D, respectively. The characteristic absorption peaks of PTB7-Th located at 276 nm, 318 nm, 631 nm and 695 nm, and the results were consistent with the literature.[11] The wide range of the absorption band of PTB7-Th indicates that it possesses good photoelectric conversion efficiency. CdTe QDs displayed a weak absorption peak around 568 nm (Figure 1D).The above results confirmed the successful preparation of PTB7-Th and CdTe QDs.

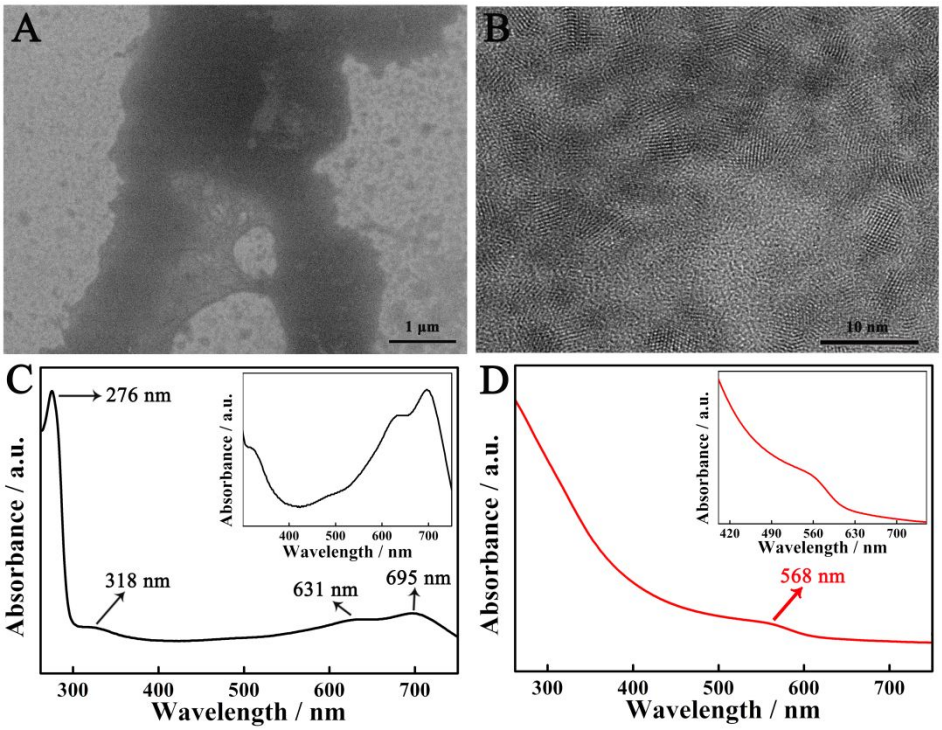

Figure 1. SEM of PTB7-Th (A); HRTEM of CdTe QDs (B); UV-vis adsorption spectrums of PTB7-Th (C) and CdTe QDs (D). The insets in (C) and (D) presented a magnification of black line in the wavelength range of 300-750 nm and a magnification of red line in the wavelength range of 410-750 nm, respectively.

The Mechanism of Electron Transfer

The mechanism of electron transfer for photocurrent generation was illustrated in Scheme 1B. Coupling the D-A type photoactive material (PTB7-Th) with the synthesized CdTe QDs to form a sensitized structure was a promising pattern for obtaining a strong initial PEC signal, which was attributed to the outstanding matching between the 1.58 eV band gap of PTB7-Th and the 1.9 eV band gap of CdTe QDs. With 460 nm light excitation, the electron of PTB7-Th migrated from its donor unit to its acceptor unit, and then transferred to the conduction band of CdTe QDs. Simultaneously, the photogenerated electron of CdTe QDs also migrated from

its valence band to its conduction band. Subsequently, the dissolved oxygen (electron acceptor) in electrolyte solution captured the photogenerated electron to form $O_2^{-\bullet}$. The continuous electron supply from the external electrode also occurred immediately. Thereby, the formed complete electron transmission path could lead to a satisfactory initial PEC signal, which profited from the sensitization effect of CdTe QDs toward PTB7-Th. Scheme 1C also presented the electron transfer process of photocurrent quenching. When target (miRNA-141) existed, miRNA-141 would be converted into DNA product *via* enzyme-assisted target cycling procedure. The acquired DNA product could trigger the formation of DNA supersanwich structure on sensing interface for loading massive MnPP. In existence of substrate H_2O_2, MnPP as the mimetic enzyme could efficiently catalyze 4-CN to generate 4-CD precipitate on electrode surface, therefrom immediately producing great steric hindrance and directly blocking the electron transmission path between the photoactive material and the electrolyte solution, leading to the significantly depressed PEC signal.

PEC Characterization of the Biosensor

Figure 2 presented the PEC responses of stepwise modified electrode. From curve a, no PEC response was obtained for bare GCE. The PEC response increased when PTB7-Th was coated on GCE surface (curve b) because of its eminent photoelectric activity. Subsequent coating with CdTe QDs, the PEC response increased significantly (curve c) owing to the effective sensitization of CdTe QDs toward PTB7-Th. When Au NPs were electrodeposited on the modified GCE surface, a further enhanced PEC response (curve d) was observed due to its admirable

conductivity. With the H2 (curve e), HT (curve f) and DNA product (curve g) continuously assembled on the above GCE surface, the PEC responses decreased successively since their charge transfer ability were poor. Ultimately, a significantly reduced PEC response was obtained (curve h) after incubated with MnPP, S1, S2, H_2O_2 and 4-CN, which contributed to the fact that MnPP as mimetic enzyme catalyzed 4-CN to generate 4-CD in existence of H_2O_2 and the electron transfer was impeded by the 4-CD precipitate. These results suggested that the stepwise construction process of this biosensor was successful.

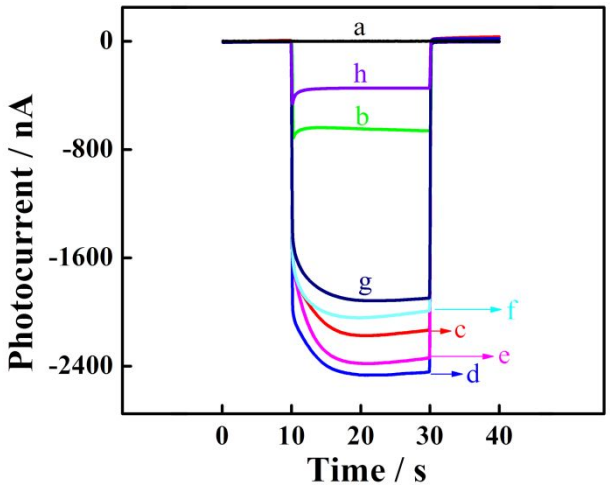

Figure 2. PEC responses of (a) bare GCE, (b) PTB7-Th/GCE, (c) CdTe QDs/PTB7-Th/GCE, (d) DepAu/CdTe QDs/PTB7-Th/GCE, (e) H2/DepAu/CdTe QDs/PTB7-Th/GCE, (f) HT/H2/DepAu/CdTe QDs/PTB7-Th/GCE, (g) DNA product/HT/H2/DepAu/CdTe QDs/PTB7-Th/GCE and (h) H_2O_2+4-CN/MnPP+S1+S2/DNA product/HT/H2/DepAu/CdTe QDs/PTB7-Th/GCE in 5 mL 0.1 M phosphate buffered solution (pH 7.4).

Detection of miRNA-141

The PEC signals toward miRNA-141 at various concentrations were recorded for investigating analytical characteristics of our PEC biosensor, in which the

measurement times for each concentration were eight times. As observed in Figure 3A, the PEC signal decreased with an increase in miRNA-141 concentrations. The PEC signals had an excellent linear relationship with the logarithm of miRNA-141 concentrations ranging from 0.1 fM to 1 nM (Figure 3B). The regression equation is $I = 122.74 \lg c - 491.38$ ($r = 0.991$), in which r, c and I are the correlation coefficient, miRNA-141 concentrations and PEC signals, respectively. Also, a low detection limit of 33 aM was derived according to the literatures.[29, 30] The detection limit and the linear range of our PEC biosensor for miRNA-141 are comparable to those of previous reports (Table 1).

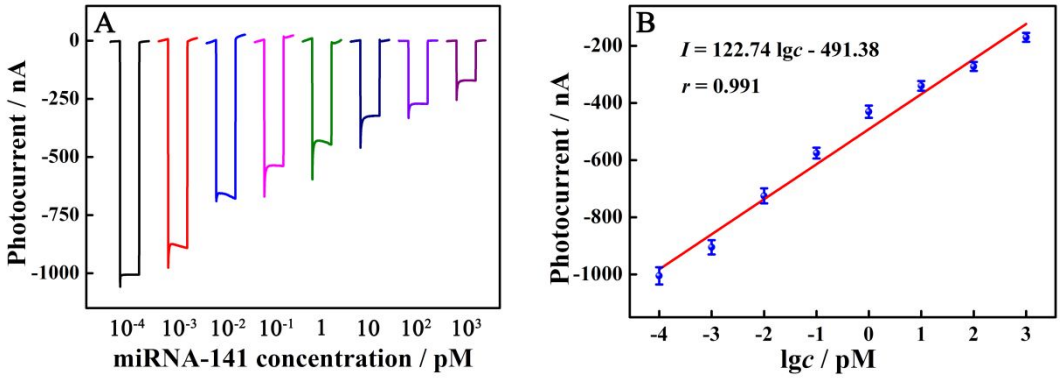

Figure 3. (A) PEC signals and (B) calibration curve for miRNA-141 detection at various concentrations.

Table 1. Comparison of different methodologies for miRNA determination.

Analytical method	Detection limit	Linear range	Ref.
fluorescence	67.3 fM	100 fM-50 pM	31
electrochemistry	2 fM	2 fM-1 nM	32
electrochemiluminescence	0.16 fM	0.5 fM-50 pM	33
PEC	83 fM	100 fM-3 nM	34
PEC	153 fM	350 fM-5 nM	35
PEC	33 aM	0.1 fM-1 nM	***Our work***

Stability and Selectivity Studies

The stability of the imprinted strategy was studied by carrying out the detection of 10 pM miRNA-141 with periodical "off-on-off" light for 8 cycles. Fairly stable PEC signals could be caught from Figure 4A when the light was turned on and the relative standard deviation (RSD) of 1.46% could be calculated, meaning that the imprinted strategy had a favorable stability. Furthermore, the selectivity of the designed strategy toward miRNA-141 was also studied through utilizing thrombin, miRNA-21 and miRNA-155 as interferents. From Figure 4B, strong PEC signals were found in existence of 1 nM interferents, which was the same as the blank detection. Nevertheless, the introduction of 10 pM miRNA-141 would lead to a weak PEC signal. The result reveals a satisfied selectivity of the designed strategy.

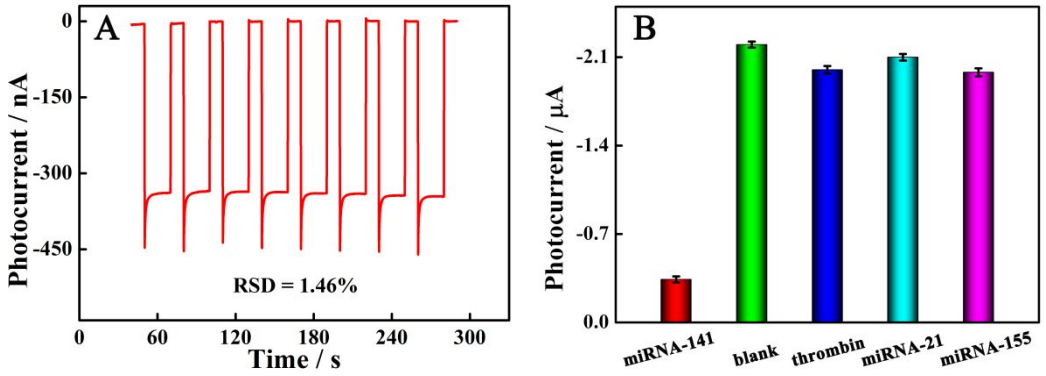

Figure 4. Stability of the proposed strategy at 10 pM miRNA-141 (A). Selectivity of the proposed strategy toward different targets: 10 pM miRNA-141, 1 nM thrombin, 1 nM miRNA-21 and 1 nM miRNA-155 (B).

Conclusions

In summary, a PEC analysis strategy was achieved using the 4-CD precipitate to efficiently quench PEC signal of the novel PTB7-Th/CdTe QDs sensitized structure

for ultrasensitive determination of miRNA-141. The PTB7-Th/CdTe QDs sensitized structure possessing preeminent photovoltaic property could create a strong initial PEC signal without any additional electron donors, which was 3.2-fold higher PEC intensity than that of alone PTB7-Th originating from the effective sensitization of CdTe QDs toward PTB7-Th. Besides, using the 4-CD precipitate as a quencher, the PEC signal of PTB7-Th/CdTe QDs sensitized structure could be significantly quenched, and the experimental results revealed that the maximum quenching percentage reached 91%. By combining DSN enzyme-assisted target cycling procedure with DNA supersanwich structure, the detection sensitivity of our designed PEC strategy has been significantly improved. More importantly, the PEC analysis strategy we developed here demonstrated great potential for the detection of various kinds of targets with great accuracy and high sensitivity.

ASSOCIATED CONTENT

Supporting Information

Materials and reagents, apparatus, PEC measurement, condition optimization (Figure S1) and electrochemical characterization of the PEC biosensor (Figure S2) were supplied in Supporting Information.

AUTHOR INFORMATION

*Corresponding authors:

Tel.: +86-23-68252277; Fax: +86-23-68253172.

E-mail address: yuanruo@swu.edu.cn (R. Yuan), yqchai@swu.edu.cn (Y. Q. Chai)

ACKNOWLEDGEMENTS

This work was financially supported by the NNSF of China (21575116, 21675129, 51473136 and 21775124) and the Fundamental Research Funds for the Central Universities (XDJK2018AA003), China.

REFERENCES

1. Wang, J.; Song, M. M.; Hu, C. G.; Wu, K. B. Portable, Self-Powered, and Light-Addressable Photoelectrochemical Sensing Platforms Using pH Meter Readouts for High-Throughput Screening of Thrombin Inhibitor Drugs. *Anal. Chem.* **2018**, *90*, 9366-9373.
2. Hou, T.; Xu, N. N.; Wang, W. X.; Ge, L.; Li, F. Truly Immobilization-Free Diffusivity-Mediated Photoelectrochemical Biosensing Strategy for Facile and Highly Sensitive MicroRNA Assay. *Anal. Chem.* **2018**, *90*, 9591-9597.
3. Zhao, W. W.; Xu, J. J.; Chen, H. Y. Photoelectrochemical Bioanalysis: the State of the Art. *Chem. Soc. Rev.* **2015**, *44*, 729-741.
4. Lan, F. F.; Liang, L. L.; Zhang, Y.; Li, L.; Ren, N.; Yan, M.; Ge, S. G.; Yu, J. H. Internal Light Source-Driven Photoelectrochemical 3D-rGO/Cellulose Device Based on Cascade DNA Amplification Strategy Integrating Target Analog Chain and DNA Mimic Enzyme. *ACS Appl. Mater. Interfaces* **2017**, *9*, 37839-37847.
5. Li, R. Y.; Tu, W. W.; Wang, H. S.; Dai, Z. H. Near-Infrared Light Excited and Localized Surface Plasmon Resonance-Enhanced Photoelectrochemical Biosensing Platform for Cell Analysis. *Anal. Chem.* **2018**, *90*, 9403-9409.
6. Hou, T.; Zhang, L. F.; Sun, X. Z.; Li, F. Biphasic Photoelectrochemical Sensing Strategy Based on in Situ Formation of CdS Quantum Dots for Highly Sensitive

Detection of Acetylcholinesterase Activity and Inhibition. *Biosens. Bioelectron.* **2016**, 75, 359-364.

7. Wu, R.; Fan, G. C.; Jiang, L. P.; Zhu, J. J. Peptide-Based Photoelectrochemical Cytosensor Using a HollowTiO_2/EG/$ZnIn_2S_4$ Cosensitized Structure for Ultrasensitive Detection of Early Apoptotic Cells and Drug Evaluation. *ACS Appl. Mater. Interfaces* **2018**, *10*, 4429-4438.
8. Zhang, G. Y.; Zhuang, Y. H.; Shan, D.; Su, G. F.; Cosnier, S.; Zhang, X. J. Zirconium-Based Porphyrinic Metal-Organic Framework (PCN-222): Enhanced Photoelectrochemical Response and Its Application for Label-Free Phosphoprotein Detection. *Anal. Chem.* **2016**, *88*, 11207-11212.
9. Sukegawa, J.; Schubert, C.; Zhu, X. Z.; Tsuji, H.; Guldi, D. M.; Nakamura, E. Electron Transfer Through Rigid Organic Molecular Wires Enhanced by Electronic and Electron-Vibration Coupling. *Nat. Chem.* **2014**, *6*, 899-905.
10. Beaujuge, P. M.; Pisula, W.; Tsao, H. N.; Ellinger, S.; Müllen, K.; Reynolds, J. R. Tailoring Structure-Property Relationships in Dithienosilole-Benzothiadiazole Donor-Acceptor Copolymers. *J. Am. Chem. Soc.* **2009**, *131*, 7514-7515.
11. Liao, S. H.; Jhuo, H. J.; Cheng, Y. S.; Chen, S. A. Fullerene Derivative-Doped Zinc Oxide Nanofilm as the Cathode of Inverted Polymer Solar Cells with Low-Bandgap Polymer (PTB7-Th) for High Performance. *Adv. Mater.* **2013**, *25*, 4766-4771.
12. Zheng, Y. N.; Liang, W. B.; Xiong, C. Y. Yuan, Y. L.; Chai, Y. Q.; Yuan, R. Self-Enhanced Ultrasensitive Photoelectrochemical Biosensor Based on

Nanocapsule Packaging Both Donor−Acceptor-Type Photoactive Material and Its Sensitizer. *Anal. Chem.* **2016**, *88*, 8698-8705.

13. Hu, T.; Zheng, Y. N.; Li, M. J.; Liang, W. B.; Chai, Y. Q.; Yuan, R. A Highly Sensitive Photoelectrochemical Assay with Donor−Acceptor-Type Material as Photoactive Material and Polyaniline as Signal Enhancer. *Anal. Chem.* **2018**, *90*, 6096-6101.
14. Zhu, H. M.; Song, N. H.; Lian, T. Q. Wave Function Engineering for Ultrafast Charge Separation and Slow Charge Recombination in Type II Core/Shell Quantum Dots. *J. Am. Chem. Soc.* **2011**, *133*, 8762-8771.
15. Crisp, R. W.; Pach, G. F.; Kurley, J. M.; France, R. M.; Reese, M. O.; Nanayakkara, S. U.; MacLeod, B. A.; Talapin, D. V.; Beard, M. C.; Luther, J. M. Tandem Solar Cells from Solution-Processed CdTe and PbS Quantum Dots Using a ZnTe-ZnO Tunnel Junction. *Nano Lett.* **2017**, *17*, 1020-1027.
16. Li, Q. Y.; Xu, Z. H.; McBride, J. R.; Lian, T. Q. Low Threshold Multiexciton Optical Gain in Colloidal CdSe/CdTe Core/Crown Type-II Nanoplatelet Heterostructures. *ACS Nano* **2017**, *11*, 2545-2553.
17. Zhu, G. Z.; Hu, R.; Zhao, Z. L.; Chen, Z.; Zhang, X. B.; Tan, W. H. Noncanonical Self-Assembly of Multifunctional DNA Nanoflowers for Biomedical Applications. *J. Am. Chem. Soc.* **2013**, *135*, 16438-16445.
18. Zhou, H.; Liu, J.; Xu, J. J.; Zhang, S. S.; Chen, H. Y. Optical Nano-Biosensing Interface via Nucleic Acid Amplification Strategy: Construction and Application. *Chem. Soc. Rev.* **2018**, *47*, 1996-2019.

19. Gerasimova, Y. V.; Kolpashchikov, D. M. Enzyme-Assisted Target Recycling (EATR) for Nucleic Acid Detection. *Chem. Soc. Rev.* **2014**, *43*, 6405-6438.

20. Zhang, H. Q.; Lai, M. D.; Zuehlke, A.; Peng, H. Y.; Li, X. F.; Le, X. C. Binding-Induced DNA Nanomachines Triggered by Proteins and Nucleic Acids. *Angew. Chem. Int. Ed.* **2015**, *54*, 14326-14330.

21. Zhang, P.; Jiang, J.; Yuan, R.; Zhuo, Y.; Chai, Y. Q. Highly Ordered and Field-Free 3D DNA Nanostructure: The Next Generation of DNA Nanomachine for Rapid Singlestep Sensing. *J. Am. Chem. Soc.* **2018**, *140*, 9361-9364.

22. Degliangeli, F.; Kshirsagar, P.; Brunetti, V.; Pompa, P. P.; Fiammengo, R. Absolute and Direct microRNA Quantification Using DNA-Gold Nanoparticle Probes. *J. Am. Chem. Soc.* **2014**, *136*, 2264-2267.

23. Chen, Y.; Wang, Q.; Xu, J.; Xiang, Y.; Yuan, R.; Chai, Y. Q. A New Hybrid Signal Amplification Strategy for Ultrasensitive Electrochemical Detection of DNA Based on Enzyme-Assisted Target Recycling and DNA Supersandwich Assemblies. *Chem. Commun.* **2013**, *49*, 2052-2054.

24. Liu, N. N.; Jiang, Y. N.; Zhou, Y. H.; Xia, F.; Guo, W.; Jiang, L. Two-Way Nanopore Sensing of Sequence-Specific Oligonucleotides and Small-Molecule Targets in Complex Matrices Using Integrated DNA Supersandwich Structures. *Angew. Chem. Int. Ed.* **2013**, *52*, 2007-2011.

25. Li, M. J.; Zheng, Y. N.; Liang, W. B.; Yuan, Y. L.; Chai, Y. Q.; Yuan, R. An Ultrasensitive ‘‘On-Off-On’’ Photoelectrochemical Aptasensor Based on Signal Amplification of a Fullerene/CdTe Quantum Dots Sensitized Structure and

Efficient Quenching by Manganese Porphyrin. *Chem. Commun.* **2016**, *52*, 8138-8141.

26. Xie, S. B.; Dong, Y. W.; Yuan, Y. L.; Chai, Y. Q.; Yuan, R. Ultrasensitive Lipopolysaccharides Detection Based on Doxorubicin Conjugated N-(Aminobutyl)-N-(ethylisoluminol) as Electrochemiluminescence Indicator and Self-Assembled Tetrahedron DNA Dendrimers as Nanocarriers. *Anal. Chem.* **2016**, *88*, 5218-5224.
27. Zhao, W. W.; Ma, Z. Y.; Yu, P. P.; Dong, X. Y.; Xu, J. J.; Chen, H. Y. Highly Sensitive Photoelectrochemical Immunoassay with Enhanced Amplification Using Horseradish Peroxidase Induced Biocatalytic Precipitation on a CdS Quantum Dots Multilayer Electrode. *Anal. Chem.* **2012**, *84*, 917-923.
28. Gong, L. S.; Dai, H.; Zhang, S. P.; Lin, Y. Y. Silver Iodide-Chitosan Nanotag Induced Biocatalytic Precipitation for Self-Enhanced Ultrasensitive Photocathodic Immunosensor. *Anal. Chem.* **2016**, *88*, 5775-5782.
29. Radi, A. E.; Sánchez, J. L. A.; Baldrich, E.; O´Sullivan, C. K. Reagentless, Reusable, Ultrasensitive Electrochemical Molecular Beacon Aptasensor. *J. Am. Chem. Soc.* **2006**, *128*, 117-124.
30. He, L.; Lu, D. Q.; Liang, H.; Xie, S. T.; Luo, G.; Hu, M. M.; Xu, L. J.; Zhang, X. B.; Tan, W. H. Fluorescence Resonance Energy Transfer-Based DNA Tetrahedron Nanotweezer for Highly Reliable Detection of Tumor-Related mRNA in Living Cells. *ACS Nano* **2017**, *11*, 4060-4066.
31. Tang, X.; Deng, R. J.; Sun, Y. P.; Ren, X. J.; Zhou, M. X.; Li, J. H. Amplified

Tandem Spinach-Based Aptamer Transcription Enables Low Background miRNA Detection. *Anal. Chem.* **2018**, *90*, 10001-10008.

32. Fang, C. S.; Kim, K. S.; Yu, B.; Jon, S.; Kim, M. S. Yang, H. Ultrasensitive Electrochemical Detection of miRNA-21 Using a Zinc Finger Protein Specific to DNA-RNA Hybrids. *Anal. Chem.* **2017**, *89*, 2024-2031.
33. Zhang, P.; Lin, Z. F.; Zhuo, Y.; Yuan, R.; Chai, Y. Q. Dual microRNAs-Fueled DNA Nanogears: A Case of Regenerated Strategy for Multiple Electrochemiluminescence Detection of microRNAs with Single Luminophore. *Anal. Chem.* **2017**, *89*, 1338-1345.
34. Liu, S. S.; Cao, H. J.; Wang, X. Y.; Tu, W. W.; Dai, Z. H. Green Light Excited Ultrasensitive Photoelectrochemical Biosensing for microRNA at a Low Applied Potential Based on the Dual Role of Au NPs in TiO_2 Nanorods/Au NPs Composites. *Nanoscale* **2018**, *10*, 16474-16478.
35. Tu, W. W.; Cao, H. J.; Zhang, L.; Bao, J. C.; Liu, X. H.; Dai, Z. H. Dual Signal Amplification Using Gold Nanoparticles-Enhanced Zinc Selenide Nanoflakes and P19 Protein for Ultrasensitive Photoelectrochemical Biosensing of MicroRNA in Cell. *Anal. Chem.* **2016**, *88*, 10459-10465.

For TOC only

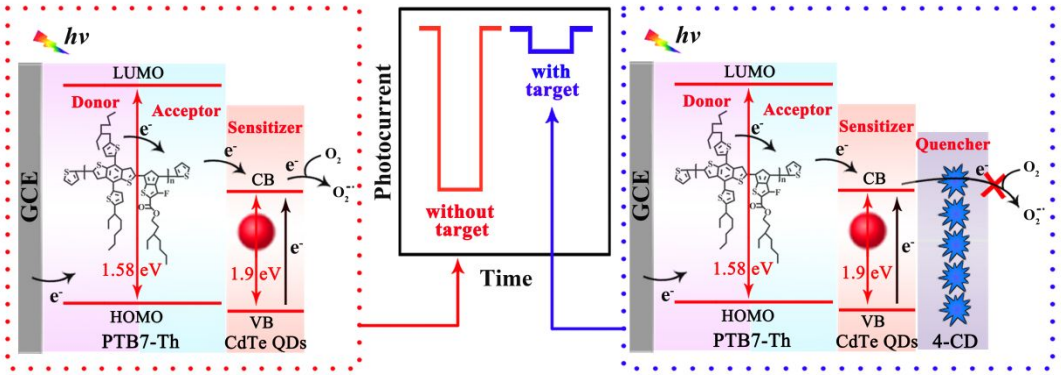
hv
LUMO
Donor
Acceptor
e-
GCE
1.58 eV
HOMO
PTB7-Th
Sensitizer
CB
1.9 eV
VB
CdTe QDs
O2
O2-
Photocurrent
with target
without target
Time
Quencher
4-CD